

Propulsive power contribution of a kite and a Flettner rotor on selected shipping routes [☆]



Michael Traut ^{a,*}, Paul Gilbert ^a, Conor Walsh ^a, Alice Bows ^{a,b}, Antonio Filippone ^a, Peter Stansby ^a, Ruth Wood ^{a,b}

^aSchool of Mechanical, Aerospace and Civil Engineering, University of Manchester, United Kingdom

^bSustainable Consumption Institute, University of Manchester, United Kingdom

HIGHLIGHTS

- Numerical models of two wind power technologies for shipping, a Flettner rotor and a towing kite, are presented.
- The methodology combines technology models and wind data along important trade routes.
- Wind power holds the potential for a step change reduction in shipping emissions.

ARTICLE INFO

Article history:

Received 9 February 2013

Received in revised form 4 June 2013

Accepted 12 July 2013

Keywords:

Shipping
Wind power
Flettner rotor
Kite
Climate change

ABSTRACT

Wind is a renewable energy source that is freely available on the world's oceans. As shipping faces the challenge of reducing its dependence on fossil fuels and cutting its carbon emissions this paper seeks to explore the potential for harnessing wind power for shipping. Numerical models of two wind power technologies, a Flettner rotor and a towing kite, are linked with wind data along a set of five trade routes. Wind-generated thrust and propulsive power are computed as a function of local wind and ship velocity. The average wind power contribution on a given route ranges between 193 kW and 373 kW for a single Flettner rotor and between 127 kW and 461 kW for the towing kite. The variability of the power output from the Flettner rotor is shown to be smaller than that from the towing kite while, due to the different dependencies on wind speed and direction, the average power contribution from a Flettner rotor is higher than that from the kite on some routes and lower on others. While for most forms of international cargo shipping wind may not be suitable as the sole source of propulsive energy, a comparison of average output to main engine power requirements of typical vessels serving the routes indicates that it could deliver a significant share. For instance, installing three Flettner rotors on a 5500 dwt general cargo carrier could, on average, provide more than half of the power required by the main engine under typical slow steaming conditions. Uncertainties and simplifying assumptions underlying the model analysis are discussed and implications of the results are considered in light of the urgent need for decarbonisation. This paper demonstrates the significant opportunities for step jump emissions reductions that wind technologies have to offer. It outlines next steps towards realising the potential, highlighting a demand for more detailed studies on socio-economic and technical barriers to implementation, and providing a basis for research into step-change emissions reductions in the shipping sector.

© 2013 The Authors. Published by Elsevier Ltd. All rights reserved.

1. Introduction

Shipping faces an enormous challenge: its fossil fuel consumption and ensuing CO₂ emissions have grown over time but in the future they must be controlled and reduced [1].

Over the three decades following the 1980s shipping crisis, both CO₂ emissions from the shipping sector and global emissions have been increasing, with international shipping emissions more than doubling between 1979 and 2009 [2] and shipping accounting for about 3% of the global total in 2007 [3]. Both are correlated to the world economy and oil prices, shipping being more volatile than global emissions. For example, due to the economic crisis beginning in 2007, international shipping emissions decreased in 2008 and even further in 2009 [2], reflecting the role of shipping as a key facilitator and beneficiary of international trade. Over periods longer than the oil price shocks and economic downturns of

[☆] This is an open-access article distributed under the terms of the Creative Commons Attribution License, which permits unrestricted use, distribution, and reproduction in any medium, provided the original author and source are credited.

* Corresponding author.

E-mail address: michael.traut@manchester.ac.uk (M. Traut).

Nomenclature

A	cross-sectional area of the Flettner rotor, 175 m ² . Area of the kite, 500 m ²	\mathbf{d}	drag force
α	denotes the spin ratio, the ratio of the rotational speed of the Flettner rotor and the apparent wind speed. $\alpha = 3.5$ in the rotor model. In the model of the kite, α denotes the angle between the negative kite velocity vector, $-\mathbf{v}_{\text{kite}}$, and the apparent wind that the kite sees, $\mathbf{v}_{\text{a,kite}}$	δ	angle between ship course and apparent wind velocity on the ship
α_{kite}	the angle α_{kite} denotes the equilibrium angle of attack: the kite moves perpendicular to the rope. If the apparent wind for the kite attacks under the angle α_{kite} , the sum of lift and drag points in the direction of the rope. $\alpha_{\text{kite}} = \arctan(C_D/C_L)$	\mathbf{l}	lift force
β	azimuthal angle between ship course and the rope if it were pointing towards the centre of the circle pattern flown by the kite. In this study, $\beta = 1/2 \cdot \delta$	lift-to-drag ratio	the ratio between the lift and a drag force on a body, given by C_L/C_D
C_D	drag coefficient (cf. Eq. (2)). Values assumed in this study: 0.2 (Flettner rotor) and 0.286 (kite)	$p_{L\&D}$	power delivered by combined lift and drag
C_L	lift coefficient (cf. Eq. (1)). Values assumed in this study: 12.5 (Flettner rotor) and 1.0 (kite)	p_{motor}	power consumed by the motor rotating the Flettner rotor
C_M	moment coefficient (cf. Eq. (3)). Value chosen in this study: 0.2 (Flettner rotor)	p_{prop}	propulsive power
		ρ	density of air; in this study $\rho = 1.2 \text{ kg/m}^3$
		\mathbf{v}_{a}	the apparent wind experienced by a body in motion, defined by the true wind velocity vector minus the body's own motion. For the ship: $\mathbf{v}_{\text{a}} = \mathbf{v}_{\text{true}} - \mathbf{v}_{\text{ship}}$, for the kite $\mathbf{v}_{\text{a}} = \mathbf{v}_{\text{true}} - \mathbf{v}_{\text{ship}} - \mathbf{v}_{\text{kite}}$, where \mathbf{v}_{kite} is relative to the ship
		$\mathbf{v}_{\text{a,kite}}$	the apparent wind seen by the kite
		\mathbf{v}_{kite}	velocity of the kite movement around the circle pattern (i.e. in the frame of reference defined by the ship)
		\mathbf{v}_{ship}	ship velocity
		\mathbf{v}_{true}	true wind, given by the wind velocity vector in the Earth system

the past decades, however, international shipping emissions have been growing steadily with growth rates outstripping those of global emissions [2,4].

For a reasonable chance to avoid dangerous climate change, global greenhouse gas emissions need to be reduced drastically [5,6]. The International Maritime Organization (IMO) recognises that, like all sectors, shipping will have to do its share [1,7,8]. Carbon reduction measures can be grouped into three categories: demand-side, operational, and technological. Constraining demand is contentious, given the relevance of shipping to international trade and the global economy, and with respect to shipping as an industry of its own right [9]. While there is scope for some improvement and optimisation in operations, e.g. where market incentives lead to inefficient practices [10] or as demonstrated by the wide-spread uptake of slow steaming (a term for reducing ship speed for the purpose of saving fuel) [11] it seems likely that technology will have to play a key role in delivering a low carbon shipping sector. Wind power technology is certainly one attractive option: wind is a free and renewable energy source that is available on the world's oceans; furthermore, it can be used in conjunction with all other low carbon fuels. The focus of this paper is to assess the potential for wind-powered shipping. The literature addressing the challenge for shipping to reduce its greenhouse gas emissions is dominated by high-level technology assessments, as in the 2nd IMO Greenhouse Gas Study [3,12,13]. Often, marginal abatement cost curves are applied as a tool for estimating the potential for emissions reductions as a function of cost under some general assumptions such as the future price of marine fuels (see [14] for an example). While covering a wide range of technologies, the emission reduction potential of a technology category is often given by a single number, sometimes per ship category, and it may be based merely on manufacturer information (cf. [3,14]). In turn, there is the perception of a large mitigation potential at negative cost, see e.g. [15], which is not realised, however. Analysing the "efficiency gap", the lack of reliable information on carbon mitigation measures is identified as a key reason for the gap [10,16]. So there is a real need for robust and openly accessible knowledge on which to base high-level assessments.

This study seeks to address the existing 'knowledge gap' in relation to the potential of wind power technology. A few studies have considered the fuel savings potential of wind power technologies analysing wind data from weather models along certain shipping lanes. In particular, Clauss et al. [17] use data from the ERA-40 database, with a resolution of $2.5^\circ \times 2.5^\circ$ from the European Centre for Medium-Range Weather Forecasts (ECMWF), to calculate fuel savings from five different sail types on three different routes. Acknowledging strong simplifications in their study, they conclude that significant savings of up to 15% at a speed of 15 knots and up to 44% at 10 knots can be made for some of the analysed ship types. They suggest the technology is cost-effective, given rising fuel costs and environmental pressures, and argue the need for more detailed analyses. Schlaak et al. [18] incorporate results from field trials with a kite into a study of the potential contribution on a network of 15 global shipping routes, using the same database. Significant fuel saving potential for a multi-purpose freighter, between 1% and 21% for a ship speed of 15 knots and between 4% and 36% for a ship speed of 13 knots, is shown. Due to time-averaging of wind speed data, they consider the result as a first order estimate.

On a similar tack, this paper introduces a numerical performance model of a Flettner rotor and one of a towing kite. They are combined with wind data from the Met Office's Unified Model with a high spatial resolution of less than 1° . A methodology for assessing the wind power contribution of the technologies towards ship propulsion is provided and applied to five different shipping routes, representing different trades, served by ships of different types and size, in different environmental conditions. In relation to the existing literature, in particular [17,18], the wind speed data used in the present paper have a higher spatial and temporal resolution. In terms of technology options, Clauss et al. [17] study various sail types, and Schlaak et al. [18] analyse a towing kite. While this study contributes to the literature by presenting a technology model of a Flettner model, the modularity of the technology model, and the inclusion of the model of a towing kite in particular, allow for the comparison of wind power technologies with different properties that operate on different mechanisms. Furthermore, the methodology stresses simplicity and modularity, high-lighting

potential power savings, rather than scoping percentage savings that depend strongly on external parameters such as ship size and type. Finally, this paper affords appropriate attention to the variability in wind power contribution which is examined in relation to the kite and Flettner rotor's different dependence on wind velocity. As a result, the methodology stands ready to be applied to any other route and to incorporate other wind power technologies such as fixed wing sails, and it serves as a starting point for more detailed studies, thus contributing towards building up the knowledge that is needed for shipping to meet the low carbon challenge.

2. Methods

The methodology comprises of three components: a numerical model of the wind power technology (Section 2.1); trade routes (Section 2.2); and wind data along those routes (Section 2.3). From these components, the potential wind power contribution is calculated as detailed in Section 2.4.

2.1. Wind power technologies

Two wind power technologies with very different properties are considered, a Flettner rotor (Section 2.1.1) and a towing kite (Section 2.1.2).

2.1.1. Flettner rotor

In the early 1920s, as an alternative to classical sails, Anton Flettner invented the Flettner rotor, an upright-mounted cylinder rotated by a motor [19]. In sideways wind the Magnus force, observed in many sports as it makes a ball with spin curve, creates a lift force that propels the ship forward (Fig. 1). A few ships were equipped with Flettner rotors and tested but the technology could not compete with steam and diesel ships at the time. Flettner rotors were reconsidered in response to the shipping crisis in the 1980s [20], and again in recent times, as focus is turning towards alternatives to fossil fuels, as indicated by a number of Computational Fluid Dynamics (CFD) studies [21,22]. In 2010, the 10,000 dwt cargo vessel E-Ship 1 was completed, equipped with four Flettner rotors of 27 m height and 4 m in diameter, demonstrating the design feasibility of the technology.

Flettner rotors are controlled via a single parameter, their rotational speed. It is assumed that the rotors are incorporated into the ship structurally as – by design – large forces are at work, and to ensure the hydrostatic and dynamic stability of the vessel.

Flettner rotors take up deck space and very likely increase the overall height of the ship, presenting potential barriers to their

installation, depending on the ship's type and intended operational profile. It is noted that these assumptions and issues need to be assessed further when considering implementing Flettner rotors on a specific vessel. All results are calculated for a single rotor. Choosing an optimum number of Flettner rotors would depend on many factors, such as vessel specifics, which are outside the scope of this study, but assumptions about the number of rotors need to be taken into account when putting results into context.

2.1.1.1. Numerical performance model. The power consumed by the motor, and the lift and drag forces acting on the cylinder determine the amount of main engine power the rotor is able to replace. The thrust gained from the rotor is calculated as the projection of the sum of the lift and drag force and, respectively, onto the course of the ship. The magnitudes of the lift and the drag force, and the power delivered by the rotor and to the rotor, respectively, are given by the following equations:

$$l = \frac{1}{2} \rho A v_a^2 C_L \quad (1)$$

$$d = \frac{1}{2} \rho A v_a^2 C_D \quad (2)$$

$$p_{L\&D} = (\mathbf{l} + \mathbf{d}) \cdot \mathbf{v}_{\text{ship}} \quad (3)$$

$$p_{\text{motor}} = \frac{1}{2} \rho A v_a^3 C_M \alpha \quad (4)$$

The defining parameters are the lift, drag, and moment coefficient, $C_L = 12.5$, $C_D = 0.2$ (in line with [21]), and $C_M = 0.2$ (in line with anecdotal evidence and preliminary CFD results, see below), respectively; the rotor is a plain cylinder, without end plates, and it has a vertical cross sectional area A , which is the height $h = 35$ m times the diameter $d = 5$ m, and the spin ratio (the ratio of the rotor surface speed and the apparent wind speed) $\alpha = 3.5$. \mathbf{v}_{ship} is the ship's velocity vector, v_a is the apparent wind speed, and ρ is the density of air. If the power contribution is smaller than that from the drag force alone it is assumed that the rotor is switched off; if the combined lift and drag force on the rotor exceeds 220 kN, corresponding to an apparent wind speed of 13 m/s, the rotor is throttled to keep both the combined lift and drag force, and the power fed into the rotor, at a constant level. The power contribution p_{prop} is calculated as the difference between the power delivered by the Flettner rotor and the power that is consumed by the motor to rotate it:

$$p_{\text{prop}} = p_{L\&D} - p_{\text{motor}} \quad (5)$$

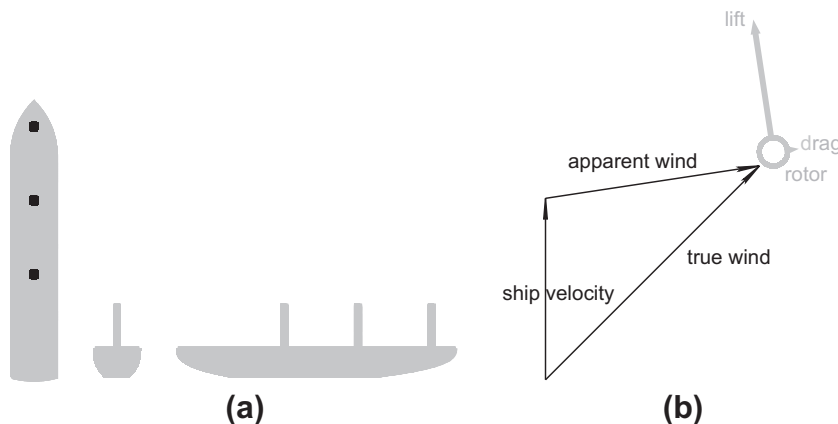


Fig. 1. Top, back, and side view of a vessel fitted with three Flettner rotors (a). Schematic of wind and ship velocity, and the resulting lift and drag force (b).

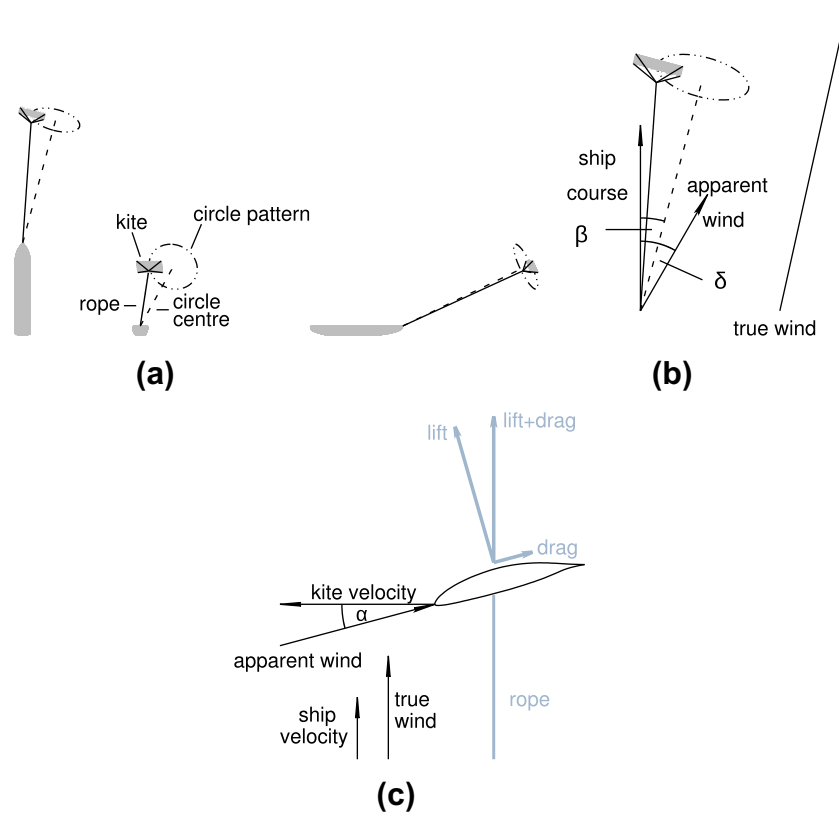


Fig. 2. Top, back, and side view of the kite and its trajectory (a). Illustration of δ , the angle between the ship course and the apparent wind, and $\beta = \delta/2$, the azimuthal angle between the ship course and the line pointing from the bow to the centre of the kite trajectory. The apparent wind on the ship is the true wind minus the ship velocity (b). The angle of the apparent wind experienced by the kite determines the direction of the aerodynamic forces on the kite (c).

2.1.1.2. Best choice of parameters. Results and, in turn, the feasibility of the Flettner rotor as a propulsion technology, hinge critically on the choice of parameters. The dimensions of the rotor and the cut-off criterion reflect design decisions, the values chosen here are in line with existing technology and anecdotal evidence,¹ and they need to be adjusted when analysing a specific case. The choice of the performance coefficients C_L , C_D , and C_M aims to estimate the values that most accurately describe the aerodynamics. Lift and drag coefficients are chosen in line with results from CFD studies [21]. Due to lack of published results, the choice of moment coefficient C_M is more difficult. The value of the moment coefficient C_M is chosen in line with anecdotal evidence (not least from Flettner himself [23]) and with initial results from CFD studies at the University of Manchester.² Finally, the aerodynamic coefficients are functions of the spin ratio α that may be chosen to control the rotor. If the functional dependencies are known exactly α can be optimised with respect to propulsive power delivered by the rotor. Here, a constant spin ratio of $\alpha = 3.5$, is assumed, reflecting a balance between maximising thrust and limiting the power expended to drive the rotor.

2.1.2. Kite

Kites may be used for power generation on land [24] and towing kites for ship propulsion have been suggested since the 1980s [25,26]. Compared to other wind power technologies, kites have some advantages: they may operate at higher altitudes where

wind speeds are often greater; they fly in front of the ship and therefore do not take up any deck space or change any of the ship's maximum dimensions; finally, they are in motion themselves, leading to higher apparent wind speeds, and consequently to higher thrust. As laid out by Loyd [24], the ideal case is that of cross-wind motion: in tail-wind conditions, the kite flies in a direction vertical to the true wind. At a certain kite speed, which is a function of the kite's lift-to-drag ratio, the sum of the lift and drag force points in the direction of the rope. As the lift and the drag force go with the square of the apparent wind speed, a large thrust is generated in this ideal case. More generally, the kite flies a pattern in front of the ship (cf. Fig. 2). At every point along the pattern the equilibrium condition is for the sum of lift and drag to point away from the ship in the direction of the rope. In favourable wind conditions it is deployed and controlled to fly along its circular trajectory. If wind conditions become unfavourable it is hauled in. Both processes are computer-controlled and fully automated. The model rests on the assumption of a towing kite that fulfils these operational criteria, without affecting the ship's stability adversely. In addition, the rope must withstand large forces.

There are already efforts in the private sector to produce and market towing kites for cargo ships [27].

2.1.2.1. Numerical performance model. The kite follows a circular trajectory in front of the ship. It pulls the ship via a rope attached to the bow, satisfying the equilibrium condition that the combined lift and drag force point in the direction of the rope. As illustrated in Fig. 2c, the equilibrium condition is met if the angle α between the negative kite velocity vector, $-\mathbf{v}_{\text{kite}}$, and the apparent wind velocity vector that the kite experiences, $\mathbf{v}_{\text{a,kite}}$, equals the kite-specific equilibrium angle of attack, α_{kite} , defined by its lift-to-drag ratio:

¹ (e.g. from Hans-Jürgen Reuß, Flettner-Rotorschiffe: Alte Technik für neue Schiffe, HANSA International Maritime Journal.)

² (McNaughton, researcher at the University of Manchester, personal communication.)

Table 1
Average power contribution of Flettner rotor and kite on the selected routes. Transient propulsion power is averaged over the course of the route and over the course of 2011. Also shown are distance, speed, and average propulsive power demand of a typical ship serving the route, assuming it is slow-steaming. Below the power demand, the ratio of power provided by a Flettner rotor and a kite, respectively, are shown. Note that while the comparison of main engine power demand and wind power contribution is illustrative, some care is needed when translating it into potential savings (cf. Section 3.4).

Route	Dunkirk to Dover (D2D)	London to Milford Haven (L2M)	Varberg to Gillingham (V2G)	Tubarao to Grimsby (T2G)	Yantian to Felixstowe (Y2F)
Flettner rotor average power contribution (kW) outgoing	338.7	193.1	206.7	200.6	246.5
Returning	372.5	205.0	222.1	200.7	250.1
Average kite power (kW) outgoing	182.3	260.0	195.3	171.0	126.7
Returning	300.1	405.8	460.6	236.3	160.3
Ship speed (m/s)	7.4	4.9	4.5	5.8	9.5
Ship speed (knots)	14.4	9.6	8.8	11.2	18.4
Ship type	RoRo	Product tanker	General cargo	Bulk carrier	Container
Dwt	7000	8000	5500	50,000	30,000
Propulsive power demand (kW) (average contribution from one Flettner rotor/a kite)	8333	1401	1014	3700	10,657
	4%/3%	14%/24%	21%/32%	5%/6%	2%/1%
Distance (km)	76	872	1093	9319	18,074

$$\alpha = \alpha_{kite} := \tan^{-1}(C_D/C_L) \quad (6)$$

The apparent wind velocity vector for the kite $\mathbf{v}_{a,kite}$ equals the true wind, \mathbf{v}_{true} , minus the ship velocity vector, \mathbf{v}_{ship} , and the kite's velocity vector tracing the circle pattern, \mathbf{v}_{kite} :

$$\mathbf{v}_{a,kite} = \mathbf{v}_{true} - \mathbf{v}_{ship} - \mathbf{v}_{kite} \quad (7)$$

At every point along the trajectory the speed of the kite is determined by the apparent wind and the kite-specific equilibrium angle of attack. The model solves for the kite speed at points spaced at 1° along the circular pattern. The thrust from the kite for a given wind and ship velocity is then calculated as the time-average (over the circular trajectory) of the projection of the rope force onto the ship course.

The lift and drag coefficients of the kite are, respectively, $C_L = 1.0$ and $C_D = 0.286$, in line with the literature (cf. e.g. [27,28]). The mass of the kite and the rope is neglected while the drag of the rope and strings holding the kite is accounted for by the choice of the drag coefficient. The equilibrium angle of attack for the kite is $\alpha_{kite} = \tan^{-1}(C_D/C_L) = 15.9^\circ$. With a kite area of $A = 500 \text{ m}^2$, the lift and drag force are given by Eqs. 1 and 2, respectively. The length of the rope is $l_{rope} = 350 \text{ m}$; the circle pattern flown by the kite has a radius of 10° , and its centre point has an elevation of 25° , both as seen from the rope's attachment point on the bow of the ship. The azimuthal angle between the ship's course and the line between the bow and the circle centre is $\beta = \delta/2$, where δ is the angle between the ship's course and the apparent wind velocity on the ship, $\mathbf{v}_{a,ship}$. The kite is deployed when it may fly satisfying its equilibrium condition at every point of the circle, the rope force does not exceed 1000 kN at any point, and $\delta < 135^\circ$.

2.1.3. Best choice of parameters

Characteristics of the kite discussed here are in line with what commercial efforts are aiming for [27,28].

With respect to the geometry of the kite pattern, no rigorous optimisation has been performed. However, many of the values are constrained by plausibility considerations and it is not expected that results would change significantly.

The engineering of ever stronger ropes is the subject of research and development, and there is no single right value to choose as a cut-off criterion with respect to maximum rope force. However, it is a critical parameter so it is important to note this criterion as an input assumption when interpreting the results. A sensitivity analysis highlights this further (cf. Section 3.3).

2.2. Routes

Five routes are selected for analysis: Yantian to Felixstowe, Tubarao to Grimsby, Varberg to Gillingham, Dunkirk to Dover,

and London to Milford Haven. All routes follow the shortest possible path, which includes passing the Strait of Malacca and the Suez Canal on the way from China to Europe. The routes provide a range of varying route distances, geographic locations (and associated wind climatologies), trades, and ship types serving the respective trades. For the purpose of this analysis, the routes are represented by a set of waypoints of coordinate pairs which are closely spaced in relation to the size of the grid cells from which the wind speed data are sampled (cf. Section 2.3). The other parameter that affects the subsequent analysis is ship speed. Ship speeds are chosen according to trade and ship types relevant for the respective route. An approximate analysis of a sample of ship movement data³ was conducted to indicate typical speeds at which ships of the type under consideration travel on the respective route. Given the premise of a strong emphasis on reducing fuel consumption, a speed reduction of 20% is assumed. Slow steaming is seen as a key element of low carbon shipping both in the literature [3,29] and within the industry [11]. While there is no single obvious choice by how much speeds should be reduced, slowing down by 20% is reasonable (cf. [29] for a quantitative discussion). Table 1 shows ship types and slow speeds applied in this analysis in knots and metres per second.

2.3. Wind data

Wind data are provided by the UK Met Office's Unified Model. The analysis data sets used provide the u (Westerly) and v (Southerly) wind speed components at various height levels on a 1024 by 769 cell grid for the u component and 1024 by 768 for the v component. At every point along the respective route, u and v are read off from the grid cell containing that point at a height level of 37 m (Flettner rotor) or 130 m (kite). Four analysis data sets are produced per day, at 0, 6, 12 and 18 h. To avoid bias through diurnal or seasonal variability, 53 data sets from the year 2011 were acquired – one every week with nearly equal numbers for each available time of day. For every wind data set (and for each technology and each route) the transient wind power contribution is calculated at every point along the route. Also, results are spatially averaged along each of the routes, and the spatial averages are averaged over time, i.e. over the 53 wind data sets.

2.4. Synthesis and power analysis

The three key elements of the presented analysis – numerical technology models, routes, and wind data – are combined to esti-

³ The research is part of the EPSRC-funded (Grant reference EP/H02011X/11) project *The High Seas* which has acquired a set of ship movement data, covering four months in 2006 worth of ship movements to and from the UK, as recorded by Lloyds List Intelligence.

mate the potential power contribution, considering the wind conditions along that route. For every set of wind data, the transient power contribution from the technology is calculated at every point along the route. Next, two averages are computed: the average wind power contribution along the route; and the power contribution on the route averaged over time. A sensitivity analysis is conducted with respect to the lift coefficient, and the moment coefficient of the Flettner rotor; and with respect to the lift and drag coefficients, and the maximal rope force of the kite.

3. Results and discussion

3.1. Flettner rotor and kite polars

Fig. 3a and b show polar plots of the power delivered by the Flettner rotor and the kite, respectively, which depend on the ship speed and the wind velocity. To be more precise: each graph (one for the rotor and one for the kite) shows ten different curves of the power as a function of the angle between the ship's course and the true wind velocity (cf. Figs. 1b and 2b). As the power is symmetric between positive and negative angles, and hence results identical, the five curves corresponding to a ship speed of 6 m/s (11.7 knots) are only plotted in the range from 0° to 180° whereas the five curves corresponding to a ship speed of 10 m/s (19.4 knots) are only plotted in the range from 180° to 360°.

The five curves differ in wind speed: the innermost is for a wind speed of 5 m/s (9.7 knots) and the outermost is for a wind speed of 15 m/s (29.2 knots). The arrow represents the course of the ship. For a straight tail wind, the distance of the curve from the origin at 0° represents the power delivered to the ship. At a ship speed of 10 m/s, and a true wind speed of 5 m/s, the apparent wind is a head wind, and in this case, the kite delivers no power to the ship. For this reason, there are only four curves in the bottom of the kite diagram, corresponding to wind speeds, of 15, 12.5, 10, and 7.5 m/s, from the outside to the inside.

There are a few points to be noted. First, power as calculated in the model is a function of the ship velocity, but not any other parameters of the ship itself, such as its size or shape (cf.

Section 3.4). The kite and the Flettner rotor show very different behaviour with respect to wind direction. The kite works well with a tail wind, in particular when the wind speed is large compared to the ship speed. The Flettner rotor, on the other hand, works particularly well for sideways winds, with the output becoming very low or even negative for a straight head or tail wind as the lift force points in the direction perpendicular to that of the ship, and the drag force dominates. In both cases, cut-off criteria apply and show in the plots: for the Flettner rotor, the cut-off is when the apparent wind speed exceeds 13 m/s, at which point the rotation rate is throttled to keep forces on the rotor constant. This explains the kinks in the curves shown in Fig. 3a. For the kite, the transient power drops to zero when the rope force exceeds 1 MN or the angle between the apparent wind and the travel direction of the ship exceeds 135°.

3.2. Power contribution on shipping lanes

Wind power – averaged spatially along the respective route and over time through the year 2011 – is given in Table 1. The power input from the Flettner rotor ranges between 193.1 kW and 372.5 kW, that from the kite between 126.7 kW and 460.6 kW when considering the five routes. The potential power contribution is highest on different routes when comparing the Flettner rotor and the kite. The average power contribution from the Flettner rotor is highest on the route Dunkirk to Dover, and on that route it is higher than the average power contribution of the kite. The reverse holds for the routes London to Milford Haven and Varberg to Gillingham.

To go beyond averages and analyse transient power input along a route in more detail, Fig. 4 shows the transient power contribution along one route, from Varberg to Gillingham: the Flettner rotor's power contribution is shown as averaged over time (Fig. 4a), on the date of lowest output (Fig. 4b), and on the date of highest output (Fig. 4c). The same results for the kite are shown in the bottom row (Fig. 4d–f). The variability in the power contribution – with respect to the different routes and different times, and between the outgoing and return leg – from the kite is much higher than that from the Flettner rotor. After considering the polar

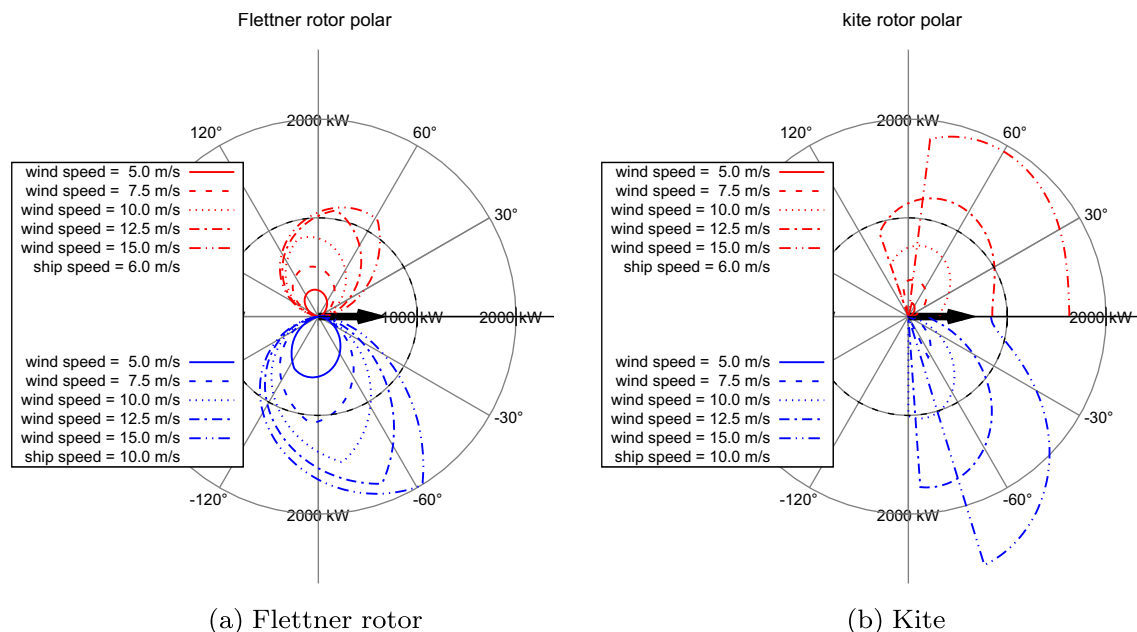


Fig. 3. Power delivered from the Flettner rotor (a) and the kite (b), as a function of the true wind angle for a ship course of 0° as indicated by the arrow; for a ship speed of 6 m/s (top half) and 10 m/s (bottom half), five different wind speeds are shown from 15 m/s (outer curve), then 12.5 m/s, 10.0 m/s, 7.5 m/s, and down to 5 m/s (inner curve). In case of the kite, the innermost curve in the bottom is zero, because the wind speed is so much lower than the ship speed. As they are naturally symmetric only one half of each curve is plotted.

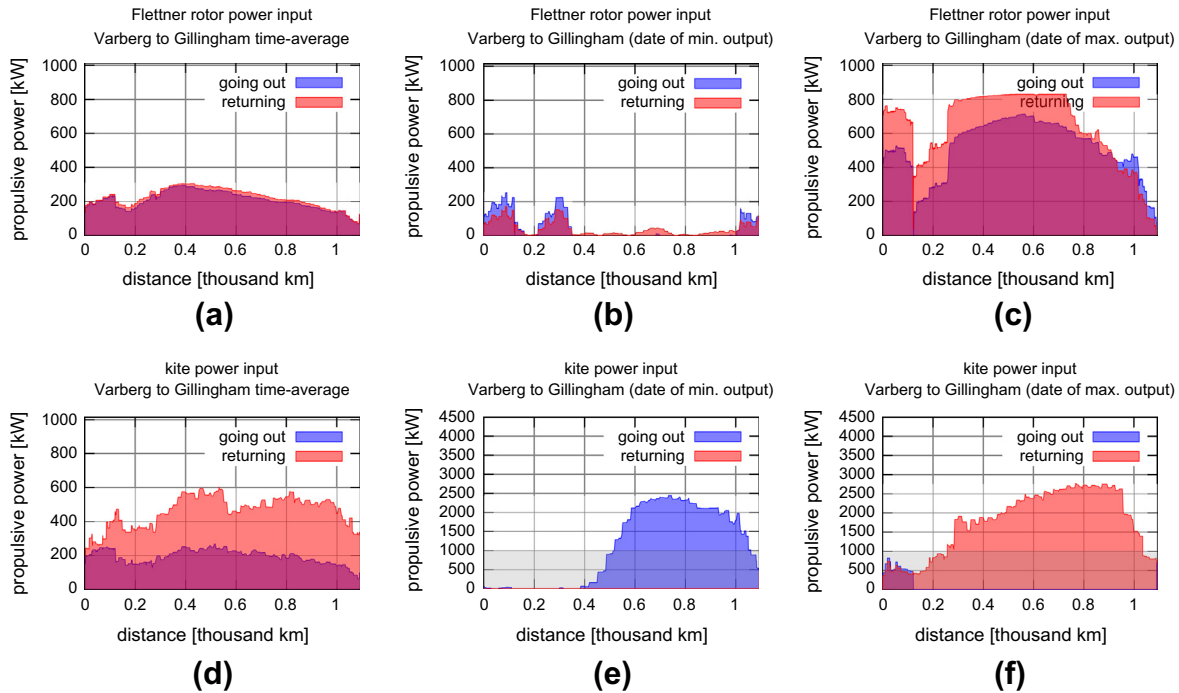


Fig. 4. Power output from the Flettner rotor (top) and the kite (bottom) along the route Varberg to Gillingham. From left to right, the average over all 53 wind data sets (a and d), on the date of minimum output (on one of the journey legs, b and e), and on the date of maximum output (on one of the journey legs, c and f) are shown. Note that where both curves overlap, the color/shading is the overlay of the two. Note the difference in scale between (a)–(d) on the one hand, and (e)–(f) on the other. To put the numbers in perspective, the y-axis range in the former corresponds to the propulsion power required by the slow steaming sample vessel serving the route (cf. Section 2.2 and Table 1); in the latter, the same range is shaded. (For interpretation of the references to colour in this figure legend, the reader is referred to the web version of this article.)

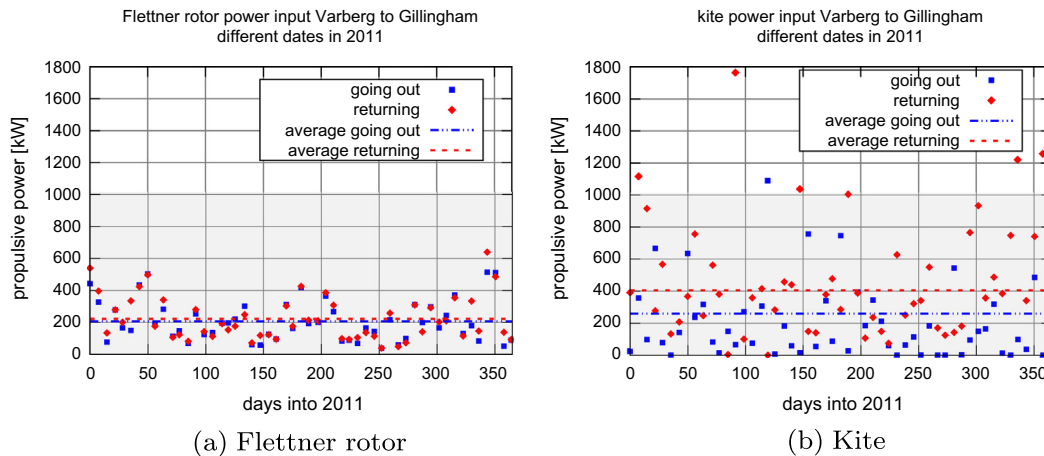


Fig. 5. Power contribution from the Flettner rotor and the kite as an average over the route Varberg to Gillingham, on all 53 sampled dates. The flat line shows the average through the year. For reference, the shaded area shows the main engine power required by the slow steaming sample ship serving the route (cf. Section 2.2 and Table 1).

graphs shown in Fig. 3a and b this is not unexpected: the Flettner rotor contributes propulsive power over a wide range of wind directions – and, in turn, geographic locations and weather conditions along the route – and the transient power contribution is similar whether going in one direction or the opposite, as Fig. 4a to c indicate. The kite, on the other hand, may deliver larger amounts of power but only if the wind is within a narrow range of directions, i.e. its performance is much more sensitive to wind speed and direction. On the date shown in Fig. 4e, the kite does not deliver any propulsive power for about the first half of the outgoing journey and none at all on the return leg. On the second half of the outgoing journey, however, its contribution is very large, of the order of 2000 kW. Fig. 5a and b show the average power contribution of the Flettner rotor and the kite, respectively, averaged

over the route Varberg to Gillingham at all points in time for which wind data were sampled, highlighting the variability of output with respect to time. Qualitatively, the same observations hold for the other routes, too. Quantitatively, the standard deviation of the results from the 53 different dates is lower for the longer routes and higher for the shorter ones, with the route Varberg to Gillingham in the middle.

3.3. Sensitivity analysis

3.3.1. Flettner rotor

The two key parameters defining the performance of a Flettner rotor are the lift coefficient C_L , determining the thrust, and the moment coefficient C_M , determining the power used to drive the rotor.

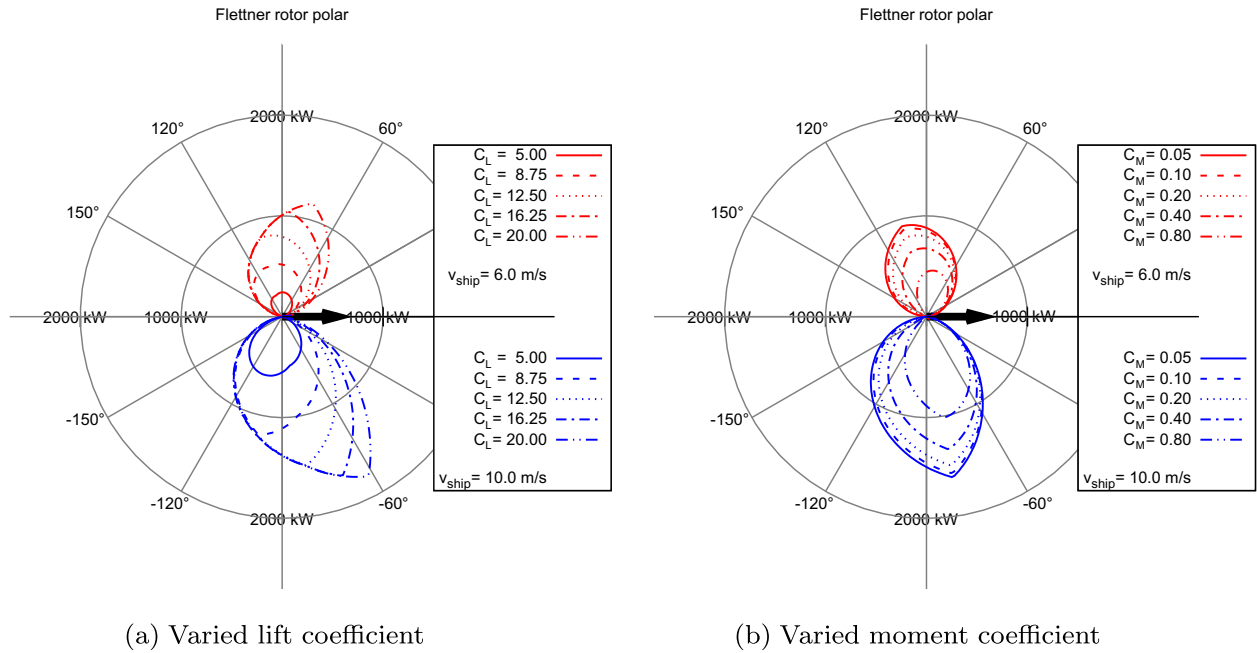


Fig. 6. Flettner rotor power for varied lift and moment coefficient. Left: Power output for lift coefficients 5.0, 8.75, 12.5, 16.25, and 20.0. Higher lift coefficients correspond to higher power output. Right: Power output for moment coefficients 0.05, 0.1, 0.2, 0.4, and 0.8. Higher moment coefficient corresponds to lower power output.

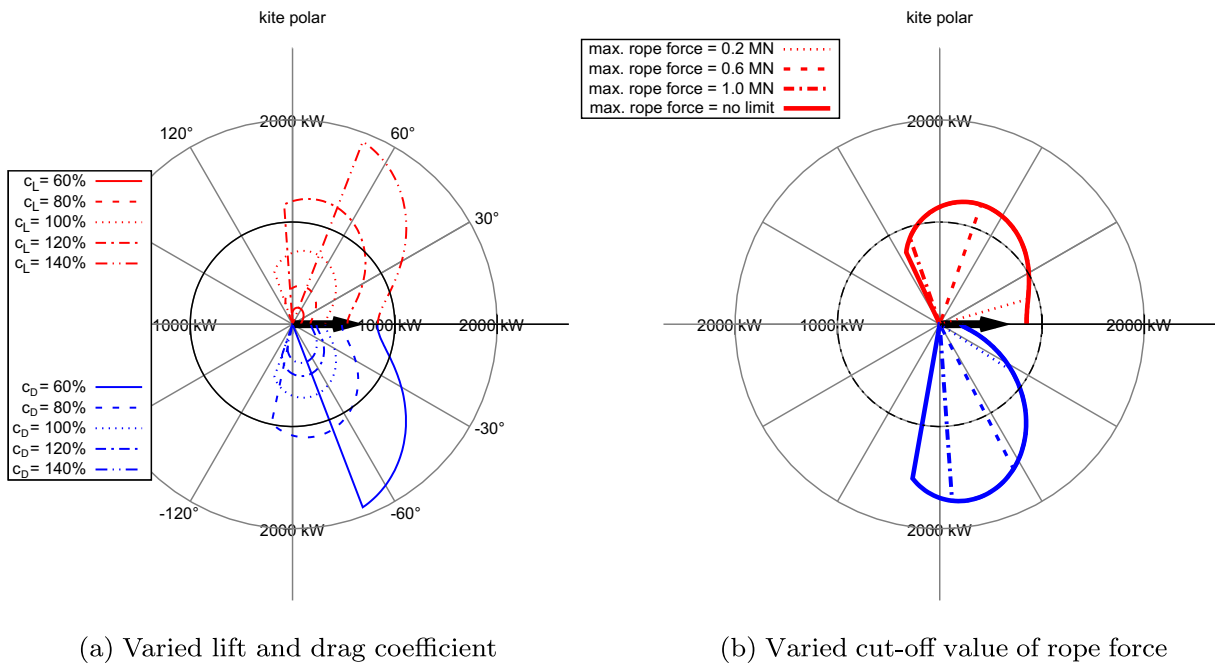


Fig. 7. Power output from the kite for varying coefficients. Left: varied lift coefficient (top half), and varied drag coefficient (bottom half), at a wind speed 10.0 m/s, and ship speed of 6 m/s. Higher lift corresponds to more power, higher drag to less power. 100% reference values are $C_L = 1.0$ and $C_D = 0.286$. Right: varied cut-off value of rope force, at a wind speed of 12.5 m/s, and ship speed of 6 m/s (top half) and 10 m/s (bottom half). Apparent wind speed is higher at larger angles between the ship course and the true wind, increasing the speed of the kite, and the force on the rope. As the cut-off is reached power output drops to zero (as the kite is retracted).

As parameters are subject to uncertainty (cf. Section 2.1.1) the power output for varying coefficient values – without the throttling criterion at high apparent wind speed – is calculated and presented in Fig. 6.

Fig. 6a and b show the power output from the Flettner rotor for varied values of the lift and moment coefficient, respectively. Increasing the lift coefficient increases the power output accordingly – in fact almost linearly (Fig. 6a). That is because the contribution from the drag force and, more importantly, the power

consumed by the rotor’s motor are comparatively small. Fig. 6b illustrates how the power output varies with the moment coefficient. A higher moment coefficient means more power is used up by the rotor, reducing power savings. For the selected value, the motor power as a fraction of the propulsion power is small and approaches zero for decreasing values. For higher moment coefficients that fraction becomes very significant – until more power is used to drive the rotor than could be saved in main engine power at which point the Flettner rotor would defeat its own purpose. In

relation to the lift coefficient (and the rotational ratio α), the moment coefficient is at a critical point. If it were much larger than assumed here it would diminish expected fuel savings significantly.

3.3.2. Kite

The key parameters in defining the power output from the kite are the lift and drag coefficients, and the constraint set by the maximum force the rope can withstand.

For a constant lift-to-drag ratio, the kite force goes linear with the lift coefficient. For a constant lift coefficient, a decreasing drag coefficient means a higher kite velocity and, in turn, a higher kite force. Fig. 7a shows how results change with the lift (top) and drag (bottom) coefficient.

In high winds, the maximum allowable force on the rope – before the kite is pulled in to avoid damage – can be a severely limiting factor. Fig. 7b shows the polar power curve of the kite at a wind speed of 12.5 m/s, for a ship travelling at 6.0 m/s (top half) and 10.0 m/s (bottom half) corresponding to four different force limits. For a given ship and wind speed, the maximum force on the rope grows with the angle between the ship course and the true wind. Therefore, curves corresponding to different force limits are the same at small angles until at some angle the curve that corresponds to the smaller force limit drops to zero as the kite is brought in. Fig. 7b illustrates how critical high performance ropes are to the concept of a towing kite.

3.3.3. Categories of uncertainty

In general, the results, as shown in Figs. 3–5 and Table 1 are subject to different types of uncertainty. First of all, the model makes assumptions regarding the technological setup, such as the size of the kite, the height of the rotor, that the technology is fully operational without significant downtime, and others. Plausible assumptions are made (cf. Section 2) but there are no single right choices. Next, the parameters used in describing the performance of the technologies, in particular the aerodynamic coefficients, are associated with uncertainty. While best estimates are chosen based on the literature (cf. Section 2), that uncertainty is not quantifiable in a straightforward manner, and therefore the most crucial parameters are the subject of the uncertainty analysis above. The wind data complementing the technology models are subject to uncertainty, being the output of a weather model and due to spatial averaging. Examining the uncertainty associated with the wind data is beyond the scope of this paper but may merit the consideration of further research. Finally, the methodology is very much an idealised representation of wind-powered propulsion as it neglects the interaction between the ship and the propulsion technology (see the following Section 3.4). That simplicity of the model reflects a balance: more specific studies will have to include such interactions but within the framework of this paper the simplicity is also a virtue with respect to ease of interpretation of the results as well as keeping them as generally applicable as possible.

3.4. Outlook: Energy analysis and optimisation

3.4.1. Energy analysis

Thrust and, in turn, propulsive power contributions, under wind conditions on-site, from a Flettner rotor and a kite, are calculated using the presented methodology. Except speed, no other vessel characteristics affect the results in the idealised model.

Results vary depending on the route analysed and potential savings may be viewed in relation to power requirements by the ship serving the route. To consider an example, on the route from Yantian to Felixstowe, representative of the Far East unitised cargo trade, the average power delivered by a kite would be of the order of 1–2% of the main engine power required by a slow-steaming

container ship of 30,000 dwt, or 2–3% for a single Flettner rotor. If more than one Flettner rotor were installed, the contribution would be expected to increase linearly until significant interference effects set in. However, on a container ship, there is also the barrier of limited deck space availability, and other markets may be more natural entry points for initial uptake.

Considering the route from Varberg to Gillingham, for a typical, slow-steaming general cargo carrier of about 5500 dwt, the average power delivered by a kite would be of the order of 20% (outgoing) to 45% (returning) of the required main engine power, or 20% (both directions) for a single Flettner rotor. Assuming an installation of three Flettner rotors, the average wind power contribution is then more than half of the main engine power demand (recalling Fig. 4a).

However, it is noted here that a few steps are needed to more realistically translate wind power contribution into fuel savings, when conducting studies focusing on a specific vessel with a given operational profile. Side slip and rudder losses introduced by any mis-alignment of the ship course and the wind-generated thrust are not considered here and, in comparing propulsive power and main engine power, transmission and propeller losses are neglected in this study. Furthermore, the main engine efficiency may change as a function of power output so its efficiency profile could be factored in. These effects partially cancel each other but need to be accounted for in more detailed analyses. Finally, these issues apply to the transient power input at any point so that the power variability along a route may play a critical role. For example, the propulsive power delivered by the kite on the way from Gillingham to Varberg may exceed the required main engine power, and care must be taken when interpreting average numbers, while noting that the Flettner rotor contribution is remarkably stable.

In order to compare results to those in the existing literature, Schlaak et al. [18] is chosen as a reference point because it too studies a towing kite. The route from Yantian to Felixstowe is similar to the Europe–Asia route in [18] and the route Tubarao to Grimsby is similar to the route Europe–Middle/South America. The kite's power contribution on the route Yantian to Felixstowe is 126.7 kW going out (160.3 kW returning) while in [18] the result on the analogous route is read from the graph as 130 kW (150 kW). On the route Tubarao to Grimsby the kite power contribution is 171.0 kW (236.3 kW), the result on the analogous route in [18] is read off as 140 kW (270 kW). Both the technology model and the wind speed data affect the results and the agreement is better than expected.

3.4.2. Optimisation

Besides applying the wind power analysis to specific vessels, trades, or even a whole fleet, the methodology may be enhanced to allow for optimisation. So far, it is assumed that ships travel on fixed routes at constant speed. However, both the exact course taken and the transient speed could be varied – while keeping the time and location of arrival fixed – to make the most of actual wind conditions and minimise fuel consumption. Regarding local weather and, more generally, environmental conditions, wind is not the only factor that has a bearing on fuel consumption: information on waves and ocean currents could be included alongside wind data to improve performance even further. Monitoring progress of wind power technology itself as well as of scientific understanding of its performance – such as aerodynamic coefficients – is an ongoing process.

3.5. Implications for decarbonisation of the shipping sector

Given that cuts to carbon emissions are imperative, and urgently required across all sectors [1], this paper raises significant

points in regard of policy development and technology road mapping. It demonstrates that even for specific technologies, the process of providing a definitive CO₂ saving per technology measure should be approached with caution. This study provides a range of 2–24% and 1–32% main engine fuel savings for a single Flettner rotor and a towing kite, respectively. If the sector is to decarbonise commensurate with the 2 °C target there is a need to define the applicability and the costs, both direct capital expenditure costs and more indirect costs such as reduced available deck space, and savings, both on the fuel bill and in emissions, of a technology measure – in this case Flettner rotors and kites – for a given vessel and route, within appropriate timeframes and scales. While this is not possible for the costs, a rough estimate of the financial savings is instructive: Considering the route from Varberg to Gillingham, a fuel price of USD 650, and a specific fuel consumption of 180 g/kWh, fitting a Flettner rotor could save about USD 600, the towing kite about USD 900 per day at sea.

On the subject of time frames, the routes and vessel types that look set to benefit the most from wind technology in the forthcoming years – relatively slow and small ships with a potential to meet a substantial share of their power requirements with wind – should be the focus of further research. From the analysed cases, a general cargo carrier serving the route between Varberg and Gillingham should be the type of example to be explored further to exploit wind power. The output of this research takes a first step towards informing deeper and wider market penetration, including other routes and ship types.

In terms of scale, this research demonstrates that considerable savings can be made on specific routes. Considering the climate change mitigation challenge, wind technology should be viewed as part of a wider shift towards a decarbonised shipping sector. Along with slow steaming and other incremental efficiency improvements, renewable propulsion technologies reduce the overall demand on the main engine. This in turn makes alternative fuels, such as sustainable biofuels or renewable synthetics, more attractive. From the more narrow view as a technology measure providing a reduction in emissions to the wider view as an element of a transition to a decarbonised sector, wind power has a step drop mitigation potential for shipping.

From a practicality perspective it should be noted that this analysis was completed along existing shipping routes – which are not necessarily optimal with respect to wind gain. With this in mind, there is arguably further potential to explore historic shipping routes and to optimise travel speeds along them. Finally, the combination of wind technologies requires further attention. The positioning and function of Flettner rotors and kites are not mutually exclusive and hence in unison could harness tail and sideways winds – resulting in increased propulsion power and CO₂ savings.

4. Conclusions

Numerical performance models of two wind power technologies, Flettner rotors and kites, are combined with wind velocity data along five shipping routes in a methodology for assessing the wind power input.

The average power contribution from the Flettner rotor on the analysed routes ranges from 193 kW to 373 kW. On the route between Varberg and Gillingham, fitting three Flettner rotors on a typical 5500 dwt, slow-steaming general cargo carrier could provide more than half of the required main engine power. Such a market could be a natural starting point for more detailed studies to establish the case for the Flettner rotor.

The average power contribution from the kite ranges from 127 kW to 461 kW; it is more volatile, both over time and geographic location, than that from a Flettner rotor and, in compar-

ison, the transient power is lower than that from two or more Flettner rotors. However, it has the advantage of taking up very little deck space, and an automated kite, subject to availability and favourable economics, is certainly a low-carbon technology option worth further consideration.

This paper shows that, although the transient power contribution is too low and variable for the industry to consider wind as the sole driver of ships typically serving the selected routes, wind can in some cases provide a major share of required propulsive power. The next steps needed in order to tap into this potential are highlighted, including modelling of the implementation of a kite and a Flettner rotor on a particular vessel with a specific pattern of operations. These studies will have to account for practical barriers and the complex integration of thrust contributions from both the main engine and the wind power technology to estimate fuel savings.

The methodology presented here provides a step towards closing the existing knowledge gap and stands ready to serve as a basis for further studies towards grasping the emission reduction opportunities presented by wind power, both as a technology providing a step drop in emissions and as an element of a wider transition to a decarbonised shipping sector.

Acknowledgements

This research is part of *The High Seas* project, funded by the EPSRC Energy Programme under Grant EP/H02011X/11. Many thanks to Brian Launder and James McNaughton for valuable support.

References

- [1] Anderson K, Bows A. Executing a Scharnow turn: reconciling shipping emissions with international commitments on climate change. *Carbon Manage* 2012;3(6):615–28.
- [2] International Energy Agency. CO₂ emissions from fuel combustion (edition: 2011); 2011.
- [3] Buhaug Ø, Corbett J, Endresen Ø, Eyring V, Faber J, Hanayama S, et al. Second IMO GHG study. London, UK: International Maritime Organization (IMO); 2009.
- [4] Endresen Ø, Sorgard E, Behrens HL, Brett PO, Isaksen ISA. A historical reconstruction of ships' fuel consumption and emissions. *J Geophys Res* 2007;112(D12):D12301. <http://dx.doi.org/10.1029/2006JD007630>.
- [5] Anderson K, Bows A. Beyond dangerous climate change: emission scenarios for a new world. *Philos Trans Roy Soc: Math Phys Eng Sci* 2011;369(1934):20.
- [6] Meinshausen M, Meinshausen N, Hare W, Raper SCB, Frieler K, Knutti R, et al. Greenhouse-gas emission targets for limiting global warming to 2 °C. *Nature* 2009;458(7242):1158–62. <http://dx.doi.org/10.1038/nature08017>.
- [7] IMO. Note by the International Maritime Organization. In: United nations framework convention on climate change – COP16; 2010.
- [8] Gilbert P, Bows A. Exploring the scope for complementary sub-global policy to mitigate CO₂ from shipping. *Energy Policy* 2012;50:613–22. <http://dx.doi.org/10.1016/j.enpol.2012.08.002>. <<http://www.sciencedirect.com/science/article/pii/S0301421512006593>>.
- [9] Walsh C, Bows A. Size matters: exploring the importance of vessel characteristics to inform estimates of shipping emissions. *Appl Energy* 2012;98:128–37. <http://dx.doi.org/10.1016/j.apenergy.2012.03.015>. <<http://www.sciencedirect.com/science/article/pii/S030626191200219X>>.
- [10] Acciaro HPN, Michele, Eide MS. The energy efficiency gap in maritime transport. In: Proceedings of the 5th maritime transport conference, technological innovation and research, Barcelona, Spain; 27th–29th June, 2012.
- [11] Woolford R, McKinnon A. The role of the shipper in decarbonising maritime supply chains. *Curr Issues Shipping, Ports Logist* 2011:11.
- [12] McCollum David L, Gould Gregory, Greene David L. Greenhouse gas emissions from aviation and marine transportation: mitigation potential and policies; UC Davis: Institute of Transportation Studies (UCD). Retrieved from: <http://escholarship.org/uc/item/5nz642qb>, 2010.
- [13] Crist P. Greenhouse gas emissions reduction potential from international shipping. OECD/ITF joint transport research centre discussion paper; 2009.
- [14] Eide M, Longva T, Hoffmann P, Endresen Ø, Dalsøren S. Future cost scenarios for reduction of ship CO₂ emissions. *Marit Policy Manage* 2011;38(1):11–37.
- [15] Longva T, Eide M, Skjong R. Determining a required energy efficiency design index level for new ships based on a cost-effectiveness criterion. *Marit Policy Manage* 2010;37(2):129–43.

- [16] Rehmatulla N, Smith T. Implementation barriers to low carbon shipping. In: Low carbon shipping 2012, Newcastle; 2012.
- [17] Clauss SH, G GF, Tampier B. Simulation of the operation of wind-assisted cargo ships. In: Hauptversammlung der Schiffbautechnischen Gesellschaft, Berlin; 21–23 November 2007.
- [18] Schlaak M, Kreutzer R, Elsner R. Simulating possible savings of the skysails-system on international merchant ship fleets. *Int J Marit Eng* 2009;151:25–37.
- [19] Flettner A. The Flettner rotor ship. *Engineering* 1925.
- [20] Bergeson L, Kent Greenwald C. Sail assist developments 1979–1985. *J Wind Eng Ind Aerodynam* 1985;19(1–3):45–114.
- [21] Craft TJ, Iacovides H, Johnson N, Launder BE. Back to the future: Flettner–Thom rotors for maritime propulsion? *Turbulence Heat Mass Transf* 2012;7.
- [22] Mittal S, Kumar B. Flow past a rotating cylinder. *J Fluid Mech* 2003;476:303–34.
- [23] Flettner A. The story of the rotor. F.O. Willhoft; 1926.
- [24] Loyd M. Crosswind kite power. *J Energy* 1980;4(3):106–11.
- [25] Duckworth R. The application of elevated sails (kites) for fuel saving auxiliary propulsion of commercial vessels. *J Wind Eng and Ind Aerodynam* 1985;20(1–3):297–315.
- [26] Wellicome J, Wilkinson S. Ship propulsive kites: an initial study. University of Southampton; 1984.
- [27] Naaijen P, Koster V, Dallinga R. On the power savings by an auxiliary kite propulsion system. *Int Shipbuild Progr* 2006;53(4):255–79.
- [28] Houska B, Diehl M. Optimal control of towing kites. In: Decision and control, 2006 45th IEEE conference on, IEEE; 2006. p. 2693–7.
- [29] Lindstad H, Asbjørnslett B, Strømman A. Reductions in greenhouse gas emissions and cost by shipping at lower speeds. *Energy Policy* 2011;39(6):3456–64. <http://dx.doi.org/10.1016/j.enpol.2011.03.044>. <<http://www.sciencedirect.com/science/article/pii/S0301421511002242>>.